Plasmonic laser with distributed feedback

Article *in* Applied Physics Letters · October 2019

DOI: 10.1063/1.5117875

CITATION
1

READS
148

7 authors, including:

Soheila Mashhadi
Norfolk State University
12 PUBLICATIONS **21** CITATIONS
SEE PROFILE

Md Omar Faruk
University of California, Irvine
8 PUBLICATIONS **25** CITATIONS
SEE PROFILE

Natalia Noginova
Norfolk State University
164 PUBLICATIONS **1,614** CITATIONS
SEE PROFILE

Applied Physics Letters

Plasmonic laser with distributed feedback

Cite as: Appl. Phys. Lett. **115**, 151103 (2019); https://doi.org/10.1063/1.5117875
Submitted: 03 July 2019 . Accepted: 23 September 2019 . Published Online: 10 October 2019

E. K. Tanyi, S. Mashhadi, C. On, Md. O. Faruk, E. Harrison, N. Noginova, and M. A. Noginov

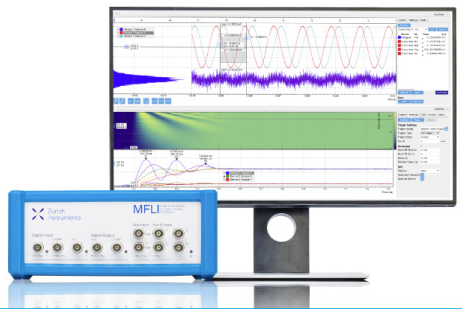

AIP Publishing

Applied Physics Letters ARTICLE scitation.org/journal/apl

Plasmonic laser with distributed feedback

Cite as: Appl. Phys. Lett. **115**, 151103 (2019); doi: 10.1063/1.5117875
Submitted: 3 July 2019 · Accepted: 23 September 2019 ·
Published Online: 10 October 2019

E. K. Tanyi,[1] S. Mashhadi,[1] C. On,[1] Md. O. Faruk,[1] E. Harrison,[2,3] N. Noginova,[1] and M. A. Noginov[1,a)]

AFFILIATIONS

[1]Center for Materials Research, Norfolk State University, Norfolk, Virginia 23504, USA
[2]Summer Research Program, Center for Materials Research, Norfolk State University, Norfolk, Virginia 23504, USA
[3]Department of Biological Sciences, University of Delaware, Newark, Delaware 19716, USA

[a)]Author to whom correspondence should be addressed: mnoginov@nsu.edu

ABSTRACT

We have demonstrated a low-threshold surface-emitting plasmonic laser radiating two symmetrical beams (at 30° from the normal to the sample) characterized by a narrow (≤1 nm) spectral width, and explained its performance in terms of the distributed feedback mechanism. The results of our study provide an extra degree of freedom to the plasmonic laser design.

Plasmonic lasers are of great interest to scientists and engineers due to their small size, which can be of the order of ∼10 nm,[1,2] and potential applications, ranging from communication[3] and nanocircuitry[4,5] to sensors[6] and biomedical imaging.[2] Lasers based on propagating surface plasmons (also known as surface plasmon polaritons, SPPs),[7–11] although less compact, have advantages over their localized plasmon counterparts (spasers)[1,2,4,12] because of a much smaller threshold gain.[13] Many such lasers, operating with and without intentional feedback, have been discussed in the literature.

Thus, in Refs. 14–18, the laser emission was supported by a distributed feedback (DFB) enabled by ordered[14–16] or (partly) disordered[17] two-dimensional (2D) arrays of plasmonic nanoparticles[14–17] or nanoholes,[18] providing highly nontrivial stimulated emission patterns.[16] The most relevant to the present study, is the plasmonic laser with the distributed feedback proposed in Ref. 19 and demonstrated in Ref. 20. In Ref. 20, the laser beam was outcoupled from the end of the DFB strip, in the plane of the grating, which required fabrication of a high-quality edge of the sample. In our work, we took one step further and demonstrated a low-threshold DFB laser emitting from the whole pumped area at the angle ∼30° relative to the normal of the surface.

In a plasmonic DFB laser, the forward and backward surface waves propagating in a periodic array of elements (which can be implemented via periodic modulation of the refractive index or the system's geometry), are coupled to each other if the vacuum wavelength, λ_0, is equal to Ref. 21

$$\lambda_0 = 2n_{sw}\Lambda/m \iff n_{sw}k_0 = \frac{m}{2}G, \tag{1}$$

where n_{sw} is the effective refractive index of the (plasmonic) surface wave, Λ is the period of the grating, G is the corresponding wavenumber, k_0, is the photon wavenumber in vacuum, and m (the Bragg's order) is an integer number. The surface plasmon (or SPP) wave with the wavenumber $n_{sw}k_0$ propagating perpendicular to the grooves of the grating can be decoupled at the angle, θ_0 given by the equation.

$$k_0 \sin(\theta_0) = n_{sw}k_0 - G, \tag{2}$$

where + and − signs in front of the terms $n_{sw}k_0$ and G were chosen to correspond to our experiment described below. (A more general equation is $k_0\sin(\theta_0) = \pm n_{sw}k_0 \pm G$.) Combining Eqs. (1) and (2), one gets

$$\sin(\theta_0) = \left(\frac{m}{2} - 1\right)\frac{G}{k_0}, \tag{3}$$

and

$$n_{sw} = \frac{m}{2}\frac{G}{k_0}. \tag{4}$$

These equations will be used at the analysis of the DFB laser described below.

The experimental samples consisted of the (i) a positive photoresist grating, deposited on top of glass using the holographic lithography technique (Λ = 583 nm), (ii) a ∼60 nm layer of Ag deposited on top of the photoresist grating, and (iii) a 3 μm layer of the poly(methyl methacrylate) (PMMA) polymer doped with the R6G laser dye, Figs. 1(a) and 1(b).

The glass substrates (2.5 cm × 2.5 cm) were cleaned in soap water, acetone, and iso-propanol (5 min. each), dried, and heated on a hot plate at 120 °C for 60 s. After that, the positive photoresist

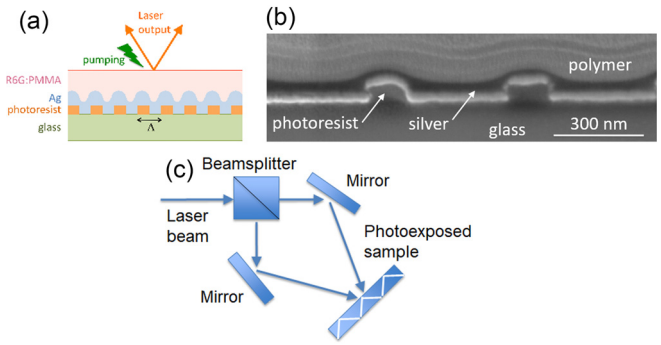

FIG. 1. (a) Schematics of the experimental sample. (b) Scanning electron microscope (SEM) image of a similar sample with different dimensions.[22] (c) Schematics of the holographic lithography setup. Figures 1(a) and 1(b) reproduced with permission from E. K. Tanyi, S. Mashhadi, C. On, M. Faruk, E. Harrison, N. Noginova, and M. A. Noginov, "Surface emitting plasmonic laser with distributed feedback," in *Conference on Lasers and Electro-Optics*, OSA Technical Digest (online) (Optical Society of America, 2018), Paper No. JTh2A.50. Copyright 2018 The Optical Society of America.

(MICROPOSIT S-1805 from Rohm and Haas Electronic Materials) was spin coated (using Spincoat G3P-8 from Specialty Coating Systems) and baked at 110 °C for 60 s. All processing of the photoresist was done in a room illuminated with yellow lamps, which did not affect the photoresist. In the holographic lithography setup, Fig. 1(c), the 325 nm beam of the HeCd laser (IK series from KIMMON) was expanded with an f = 2.5 cm concave lens, split into two channels (~2.9 mW in each) using a nonpolarizing 50/50 cube beam splitter, and then recombined on the glass slide coated with the photoresist. After 30 s photoexposure, the photoresist was developed for 30 s (in the MF 319 developer from Rohm and Haas Electronic Materials), the sample was rinsed in distilled water and baked at 110 °C for 60 s, leaving a well-developed grating of dielectric photoresist strips, see the sample schematics [Fig. 1(a)] and the scanning electron microscope (SEM) image of a sample prepared by a similar method, but with slightly different dimensions [Fig. 1(b)]. The period of the fabricated grating, $\Lambda = 583$ nm, determined by measuring the angle corresponding to the first order of diffraction of the 568.2 nm Kr laser light, agreed with that calculated based on the angle between the two 325 nm HeCd laser beams.

By thermally depositing ~60 nm of silver (using NANO 36 thermal evaporator from Kurt J. Lesker) on top of the dielectric grating, we obtained a metallic grating, whose bottom surface was conformal to the photoresist grating and the top surface was nearly sinusoidal. Finally, we spin coated on top of the silver grating a 3 μm thick film of poly(-methyl methacrylate) (PMMA) doped by rhodamine 6G (R6G) dye in a concentration of 6.0×10^{-2} mol/l (equivalent to 28.7 g/l, in the solid-state or 3.97×10^{19} cm^{-3}). The preparation of the R6G:PMMA film is discussed in detail in Ref. 23. The thickness of Ag and R6G:PMMA films as well as the depth of the photoresist grating were characterized using a DekTak XT profilometer (from Bruker). The top surface of the R6G:PMMA layer, examined with AFM, was flat with ±3 nm accuracy. Two nominally identical grating-based samples were fabricated and studied experimentally, showing a nearly similar behavior. The results presented below have been obtained in one of these samples. The control samples were ~3 μm R6G:PMMA films (6.0×10^{-2} mol/L) deposited onto the 80 nm Ag film on the glass substrate.

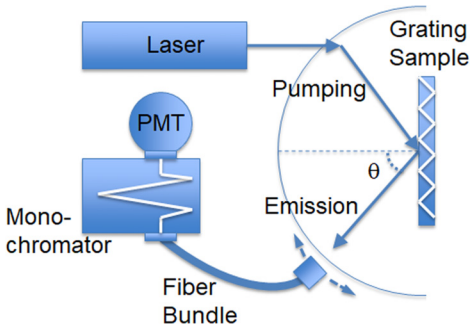

FIG. 2. Schematics of the experimental setup used in the studies of spontaneous and stimulated emission.

The samples were pumped with ~10 ns pulses of the frequency doubled Q-switched Nd:YAG laser at $\lambda = 532$ nm (Quanta-Ray, model GCR-170 from Spectra-Physics). The laser beam was lightly focused to a spot with an area of 0.06 cm^2. The emission was collected at normal to the sample (Fig. 2) and directed to the input slit of a monochromator (MS257 from Newport/Oriel). The latter was equipped with a 550 nm long-pass filter to remove residual pumping light. In some measurements, a plastic sheet polarizer was used to transmit TM or TE polarized light. The signal was detected with a photomultiplier tube (PMT, R5108 from Hamamatsu), attached to the monochromator's output slit and processed using a combination of a boxcar integrator (Stanford Research Systems SR250) and a lock-in amplifier (Merlin, Newport/Oriel), Fig. 2. The spectral scans were collected and recorded using the TraqQ software (Newport/Oriel).

At a small pumping density (≤ 0.45 mJ/cm^2), the spontaneous emission spectrum of the R6G:PMMA film on top of the grating sample (measured at normal to the sample surface) had the maximum at 586 nm, Fig. 3(a). The angular distribution of spontaneous emission had two maxima, at ~30° on both sides of the normal to the sample, almost the same in vertical (TE) and horizontal (TM) polarizations, Fig. 3(b).

The series of unpolarized emission spectra recorded at several gradually increasing pumping energies, in the direction normal to the sample's surface (Fig. 4, dashed traces), shows transformation from the spontaneous emission to the predominantly stimulated emission, which is manifested by the growth of the $\lambda = 601$ nm peak. This

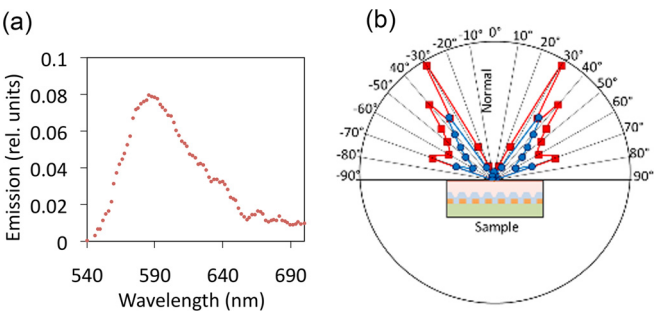

FIG. 3. Spontaneous emission of the grating sample at weak pumping. (a) Emission spectrum (unpolarized). (b) Angular distribution in TE polarization (red squares) and TM polarization (blue circles) emission intensity.

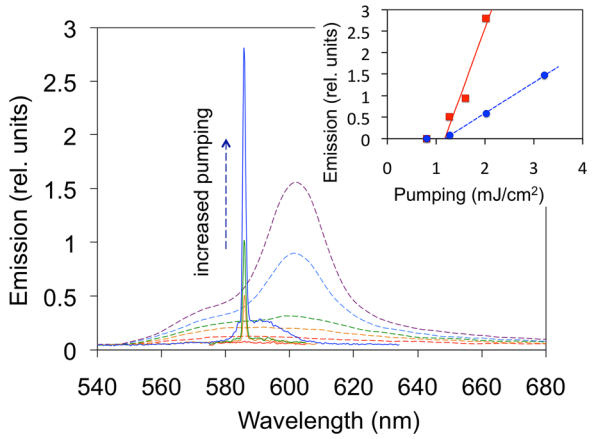

FIG. 4. The series of emission spectra recorded in TM polarization at several pumping energies at the position of the laser spot (solid lines) and unpolarized emission at the direction normal to the grating surface (dashed lines). Inset: corresponding input-output curves measured at the laser spot (red squares) and at the normal direction (blue circles). Figure 4 reproduced with permission from E. K. Tanyi, S. Mashhadi, C. On, M. Faruk, E. Harrison, N. Noginova, and M. A. Noginov, "Surface emitting plasmonic laser with distributed feedback," in *Conference on Lasers and Electro-Optics*, OSA Technical Digest (online) (Optical Society of America, 2018), Paper No. JTh2A.50.

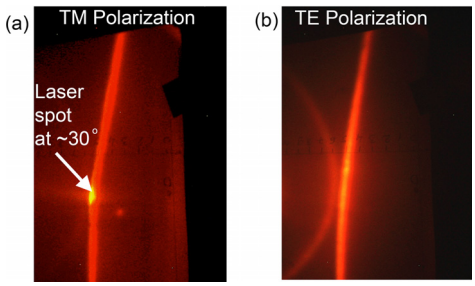

FIG. 5. (a) Laser spot on the white screen, recorded in TM polarization at $\theta_0 \sim 30°$ from the normal to the sample. (b) Photograph of the same screen in TE polarization does not show any laser spot. Figures 5(a) and 5(b) reproduced with permission from "E. K. Tanyi, S. Mashhadi, C. On, M. Faruk, E. Harrison, N. Noginova, and M. A. Noginov, "Surface emitting plasmonic laser with distributed feedback," in *Conference on Lasers and Electro-Optics*, OSA Technical Digest (online) (Optical Society of America, 2018), Paper No. JTh2A.50.

emission is nearly polarization independent and its relatively large spectral width is consistent with the stimulated emission without intentional feedback (or amplified spontaneous emission, ASE), which can originate from both (i) SPPs scattered by unintentional defects or (ii) the volume of the dye-doped polymer, which was unaffected by SPPs.

To separate spontaneous and stimulated contributions to the overall emission spectra, we scaled the purely spontaneous emission spectrum recorded at a small pumping density [0.45 mJ/cm^2, Fig. 3(a)] to match the ~586 nm spontaneous emission in each of the spectra recorded at stronger pumping and subtracted the former from the latter. This procedure allowed us to single out the ASE emission band, whose magnitude, plotted against the pumping density, resulted in the input-output curve depicted in the inset of Fig. 4, blue circles.

At the pumping density exceeding 1.2 mJ/cm^2, we have observed two narrow laser beams propagating at the angle $\theta_0 \sim 30°$, on both sides of the normal to the sample surface. Their well-defined slightly elongated spots had yellowish color that was distinctly different from the orange ASE background, Fig. 5. The corresponding spectral line was ~1 nm wide (determined by the slits of the monochromator) and had a maximum at 585.5 nm—nearly 15 nm away from the maximum of the ASE band, Fig. 4. This emission was purely TM polarized [compare Figs. 5(a) and 5(b)], which is consistent with its surface plasmon origin. By recording a series of emission spectra corresponding to different pumping powers, we were able to plot the input-output curve (inset of Fig. 4) and evaluate the threshold pumping density, 1.2 mJ/cm^2, which was very close to that of the broad-band stimulated emission recorded in the normal direction and nearly six times smaller than the threshold pumping density reported in the DFB plasmonic laser in Ref. 20. The arching lines seen on the screen next to the laser spot [Figs. 5(a) and 5(b)] are due to diffraction of the partly coherent ASE emission by the grating—the phenomenon, whose detailed study will be reported elsewhere. The well-defined laser beam and the narrow spectral line (whose spectral position is noticeably different from the maximum of the gain band and ASE) are indicative of the stimulated emission with feedback and well-defined laser modes. (The latter is likely responsible for the wavelength selectivity and the 15 nm shift between the narrow laser line and the maximum of the ASE band. More generally, the wavelength of the dye emission out-coupled, at angle θ_0, by SPPs supported by a metallic grating [Eq. (3)] is expected to be different from the wavelength of emission, recorded in the direction normal to the sample's surface, that was not coupled with SPPs or scattered by the sample's imperfections.)

Note that the evolution of the emission spectra with an increase in the pumping density, qualitatively similar to that depicted by dashed lines in Fig. 4, was observed in the silver-based control sample without grating. However, the latter did not produce any laser beams.

The coherence of the laser radiation was examined using the home-built Michelson interferometer, Fig. 6(a). The visibility of the interference pattern (calculated as $v = (I_{max} - I_{min})/(I_{max} + I_{min})$, where I_{max} and I_{min} are the maximal and minimal intensities) was equal to $\nu = 0.62$ [Figs. 6(b) and 6(c)], nearly the same as that of the frequency doubled Nd:YAG pumping laser (Quanta-Ray, model GCR-170 from Spectra-Physics) measured in the same setup, $\nu = 0.63$. (The relatively low visibility was probably due to a slight imbalance of the intensities of the two beams.)

The longitudinal coherence length is given by $L_c = c\tau_c = A\lambda^2/\Delta\lambda$, where τ_c is the coherence time, c is the speed of light, $\Delta\lambda$ is the spectral linewidth, and the coefficient A (of the order of unity) depends on the nature of the broadening.[24] Given $\lambda = 585.5$ nm and $\Delta\lambda \leq 1$ nm, the coherence length is $L_c \geq 3.4 \times 10^{-2}$ cm (assuming A = 1). Since $\Delta\lambda$ is limited by the slits of the monochromator (1 nm), L_c is expected to be even larger.

By substituting the experimental values of G, k_0, and θ_0 into Eq. (3), we have determined m = 3.00, which is very close to integer 3. Assuming that the surface wave is an SPP, we find from Eq. (4), $n_{sw} = 1.50$. However, at $\lambda_0 = 585.5$ nm, the refractive index of the SPP wave is equal to $n_{sw} = \sqrt{\varepsilon_m \varepsilon_d/(\varepsilon_m + \varepsilon_d)} = 1.62$. Here, ε_m is the dielectric permittivity of Ag[25] and ε_d is that of the dye-doped PMMA.[26] The latter modest discrepancy can be explained by the fact that the values of dielectric permittivities in our experimental sample

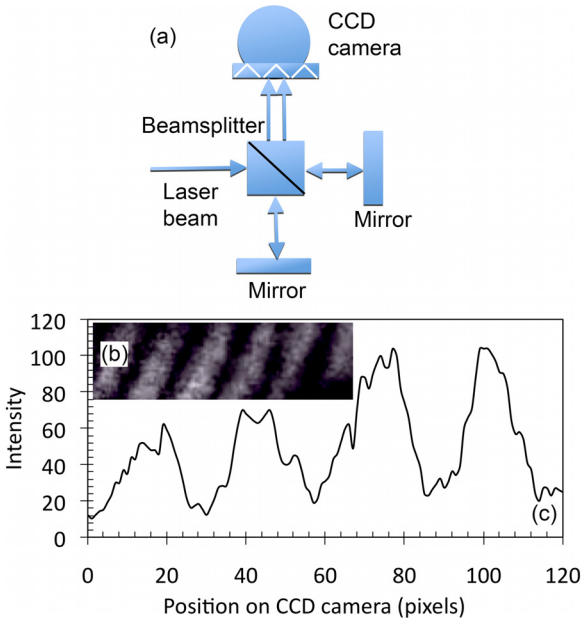

FIG. 6. (a) Schematics of the Michelson interferometer setup. (b). The interference pattern. (c) The intensity profile for the DFB plasmonic laser, $\lambda = 585.5$ nm.

slightly deviated from those known in the literature. Alternatively, the surface wave might not be a pure SPP but rather a hybrid SPP-related mode supported by a waveguide formed by the Ag grating on one side and the polymer/air interface on the other side.

On the other hand, at high R6G dye concentration used in this study, excitons in ensembles of dye molecules and surface plasmon polaritons (SPPs) strongly couple to each other, resulting in the Rabi splitting of the dispersion curve and formation of the polariton spectral bands.[27] This coupling can potentially explain the modest mismatch discussed above.

A broad range of emission outcoupling angles can be realized if m, n_{sw}, k_0, and G are used as design parameters [Eqs. (3) and (4)]. Thus, θ_0 is equal to zero at m = 2. At other Bragg orders m, the emission angle can be controlled by the vacuum wavelength λ_0 or the grating period Λ, which are related to each other, as well as to m and n_{sw}, by Eq. (4). The parameters λ_0 and n_{sw} are determined by the choice of the dye, the metal, and the polymer.

Note that all-dielectric thin film dye lasers with a distributed feedback have been extensively discussed in the literature.[28–31] Some of them, which employed R6G dye,[28,29,31] emitted normally to the surface (at Bragg order m = 2)[29,30] and their stimulated emission lines were blue shifted in comparison to broad spectral bands of gain and ASE.[30,31] (The third Bragg order, similar to that in our study, was used in the DFB laser reported in Ref. 31.) However, their stimulated emission was TE polarized, in striking difference with TM polarized laser light in the plasmonic DFB laser reported here. The potential advantage of plasmonic lasers over purely dielectric photonic lasers is the high speed of modulation.[4,32]

To summarize, we have demonstrated a low-threshold grating-based plasmonic laser emitting two symmetrical beams (at 30° from the normal to the sample), which were characterized by a narrow (≤1 nm) spectral width. We explained the laser performance in terms of the distributed feedback mechanism. The results of our study provide an extra degree of freedom to the plasmonic laser design.

This work was supported by NSF Grant Nos. 1646789, 1830886, and 1856515, AFOSR Grant No. FA9550-18-1-0417, and DoD Grant No. W911NF1810472. The authors cordially thank S. D. Bhattacharyya, T. Galfsky, and V. Menon at the City University of New York for taking the SEM image of the sample.

REFERENCES

[1]M. A. Noginov, G. Zhu, A. M. Belgrave, R. Bakker, V. M. Shalaev, E. E. Narimanov, S. Stout, E. Herz, T. Suteewong, and U. Wiesner, "Demonstration of a spaser-based nanolaser," Nature **460**, 1110 (2009).
[2]E. I. Galanzha, R. Weingold, D. A. Nedosekin, M. Sarimollaoglu, J. Nolan, W. Harrington, A. S. Kuchyanov, R. G. Parkhomenko, F. Watanabe, Z. Nima *et al.*, "Spaser as a biological probe," Nat. Commun. **8**, 15528 (2017).
[3]J. Leuthold, C. Hoessbacher, S. Muehlbrandt, A. Melikyan, M. Kohl, C. Koos, W. Freude, V. W. Dolores Calzadilla, M. K. Smit, I. Suarez *et al.*, "Plasmonic communications: Light on a wire," Opt. Photonics News **24**, 28 (2013).
[4]M. I. Stockman, "The spaser as a nanoscale quantum generator and ultrafast amplifier," J. Opt. **12**, 024004 (2010).
[5]T. W. Ebbesen, C. Genet, and S. I. Bozhevolnyi, "Surface plasmon circuitry," Phys. Today **61**(5), 44 (2008).
[6]W. Zhu, T. Xu, H. Wang, C. Zhang, P. B. Deotare, A. Agrawal, and H. J. Lezec, "Surface plasmon polariton laser based on a metallic trench Fabry-Perot resonator," Sci. Adv. **3**, e1700909 (2017).
[7]A. N. Sudarkin and P. A. Demkovich, "Excitation of surface electromagnetic waves on the boundary of a metal with an amplifying medium," Sov. Phys. Tech. Phys. **34**, 764 (1989).
[8]M. A. Noginov, G. Zhu, M. Mayy, B. A. Ritzo, N. Noginova, and V. A. Podolskiy, "Stimulated emission of surface plasmon polaritons," Phys. Rev. Lett. **101**, 226806 (2008).
[9]R. F. Oulton, V. J. Sorger, T. Zentgraf, R.-M. Ma, C. Gladden, L. Dai, G. Bartal, and X. Zhang, "Plasmon lasers at deep subwavelength scale," Nature **461**, 629 (2009).
[10]J. K. Kitur, V. A. Podolskiy, and M. A. Noginov, "Stimulated emission of surface plasmon polaritons in a microcylinder cavity," Phys. Rev. Lett. **106**, 183903 (2011).
[11]J. K. Kitur, L. Gu, T. Tumkur, C. Bonner, and M. A. Noginov, "Stimulated emission of surface plasmons on top of metamaterials with hyperbolic dispersion," ACS Photonics **2**(8), 1019 (2015).
[12]D. J. Bergman and M. I. Stockman, "Surface plasmon amplification by stimulated emission of radiation: Quantum generation of coherent surface plasmons in nanosystems," Phys. Rev. Lett. **90**(2), 027402 (2003).
[13]M. A. Noginov, in *Metamaterials and Plasmonics With Optical Gain*, Handbook of Metamaterials Properties—Volume 3. Active Nanoplasmonics and Metamaterials, edited by S. A. Maier (World Scientific Publishing Company, 2017).
[14]J. Stehr, J. Crewett, F. Schindler, R. Sperling, G. von Plessen, U. Lemmer, J. M. Lupton, T. A. Klar, J. Feldmann, A. W. Holleitner *et al.*, "A low threshold polymer laser based on metallic nanoparticle gratings," Adv. Mater. **15**, 1726 (2003).
[15]W. Zhou, M. Dridi, J. Y. Suh, C. H. Kim, D. T. Co, M. R. Wasielewski, G. C. Schatz, and T. W. Odom, "Lasing action in strongly coupled plasmonic nanocavity arrays," Nat. Nanotechnol. **8**, 506 (2013).
[16]A. H. Schokker and A. F. Koenderink, "Lasing at the band edges of plasmonic lattices," Phys. Rev. B **90**, 155452 (2014).
[17]A. H. Schokker and A. F. Koenderink, "Statistics of randomized plasmonic lattice lasers," ACS Photonics **2**, 1289 (2015).
[18]F. van Beijnum, P. J. van Veldhoven, E. J. Geluk, M. J. A. de Dood, G. W. 't Hooft, and M. P. van Exter, "Surface plasmon lasing observed in metal hole arrays," Phys. Rev. Lett. **110**, 206802 (2013).
[19]E. K. Keshmarzi, R. N. Tait, and P. Berini, "Long-range surface plasmon single-mode laser concepts," J. Appl. Phys. **112**, 063115 (2012).

[20]E. K. Keshmarzi, R. N. Tait, and P. Berini, "Surface plasmon distributed feedback lasers," paper presented at Physics of Quantum Electronics, Snowbird, Utah, USA, 8–13 January, 2017.
[21]O. Svelto, *Principles of Lasers* (Springer, 2010).
[22]S. D. Bhattacharyya, T. Galfsky, and V. Menon, at the City University of New York for taking SEM image of the sample.
[23]E. K. Tanyi, H. Thuman, N. Brown, S. Koutsares, V. A. Podolskiy, and M. A. Noginov, "Control of stokes shift with strong coupling," Adv. Opt. Mater. **5**, 1600941 (2017).
[24]M. V. Klein and T. E. Furtak, *Optics*, 2nd ed. (Wiley, 1986).
[25]P. B. Johnson and R. W. Christy, "Optical constants of the noble metals," Phys. Rev. B **6**(12), 4370 (1972).
[26]N. Sultanova, S. Kasarova, and I. Nikolov, "Dispersion properties of optical polymers," Acta Phys. Polonica A **116**, 585 (2009).
[27]T. U. Tumkur, G. Zhu, and M. A. Noginov, "Strong coupling surface plasmon polaritons and ensembles of dye molecules," Opt. Express **24**(4), 3921 (2016).
[28]M. Maeda, Y. Oki, and K. Imamura, "Ultrashort pulse generation from an integrated single-chip dye laser," IEEE J. Quantum Electron. **33**, 2146 (1997).
[29]T. Kobayashi, Y. Kanamori, and K. Hane, "Surface laser emission from solid polymer dye in a guided mode resonant grating filter structure," Appl. Phys. Lett. **87**, 151106 (2005).
[30]D. Schneider, S. Hartmann, T. Benstem, T. Dobbertin, D. Heithecker, D. Metzdorf, E. Becker, T. Riedl, H.-H. Johannes, W. Kowalsky *et al.*, "Wavelength-tunable organic solid-state distributed-feedback laser," Appl. Phys. B **77**, 399 (2003).
[31]W. Horn, S. Kroesen, and C. Denz, "Two-photon fabrication of organic solid-state distributed feedback lasers in rhodamine 6G doped SU-8," Appl. Phys. B **117**, 311 (2014).
[32]J. B. Khurgin and G. Sun, "Comparative analysis of spasers, vertical-cavity surface-emitting lasers and surface-plasmon-emitting diodes," Nat. Photonics **8**, 468 (2014).